Microbiome

RESEARCH Open Access

Bikaverin as a molecular weapon: enhancing *Fusarium oxysporum* pathogenicity in bananas via rhizosphere microbiome manipulation

Honglin Lu[1†], Suxia Guo[2†], Yongbao Yang[1], Zhihao Zhao[1], Qingbiao Xie[1], Qiong Wu[2], Changjun Sun[2], Hongli Luo[1], Bang An[1*] and Qiannan Wang[1*]

Abstract

Background *Fusarium* wilt, caused by *Fusarium oxysporum* f. sp. *cubense* Tropical Race 4 (Foc TR4), poses a severe threat to global banana production. Secondary metabolites are critical tools employed by pathogens to interact with their environment and modulate host–pathogen dynamics. Bikaverin, a red-colored polyketide pigment produced by several *Fusarium* species, has been studied for its pharmacological properties, but its ecological roles and impact on pathogenicity remain unclear.

Results This study investigated the role of bikaverin in Foc TR4, focusing on its contribution to pathogenicity and its interaction with the rhizosphere microbiome. Pathogenicity assays under sterile and autoclaved conditions demonstrated that bikaverin does not directly contribute to pathogenicity by affecting the infection process or damaging host tissues. Instead, bikaverin indirectly enhances Foc TR4's pathogenicity by reshaping the rhizosphere microbiome. It suppresses beneficial plant growth-promoting rhizobacteria, such as *Bacillus*, while promoting the dominance of fungal genera, thereby creating a microbial environment beneficial for pathogen colonization and infection. Notably, bikaverin biosynthesis was found to be tightly regulated by environmental cues, including acidic pH, nitrogen scarcity, and microbial competition. Co-culture with microbes such as *Bacillus velezensis* and *Botrytis cinerea* strongly induced bikaverin production and upregulated expression of the key bikaverin biosynthetic gene *FocBik1*. In addition, the identification of bikaverin-resistant *Bacillus* BR160, a strain with broad-spectrum antifungal activity, highlights its potential as a biocontrol agent for banana wilt management, although its stability and efficiency under field conditions require further validation.

Conclusions Bikaverin plays an indirect yet important role in the pathogenicity of Foc TR4 by manipulating the rhizosphere microbiome. This ecological function underscores its potential as a target for sustainable disease management strategies. Future research should focus on elucidating the molecular mechanisms underlying bikaverin-mediated microbial interactions, using integrated approaches such as transcriptomics and metabolomics. Together, these findings provide a foundation for novel approaches to combat banana wilt disease and enhance crop resistance.

[†]Honglin Lu and Suxia Guo contributed equally to this work.

*Correspondence:
Bang An
anbang@hainanu.edu.cn
Qiannan Wang
wangqiannan@hainanu.edu.cn
Full list of author information is available at the end of the article

Keywords Banana wilt disease, Foc TR4, Secondary metabolites, Bikaverin, Rhizosphere microbiome, Plant growth-promoting rhizobacteria, *Bacillus*

Background

Banana (*Musa spp.*) ranks as one of the most important crops worldwide, serving as a staple food for millions. In 2023, the global banana market reached an export volume of 19.3 million tonnes (FAO, 2024). Despite its significance, banana cultivation faces a severe threat from *Fusarium* wilt, also known as "Panama disease," caused by the soil-borne fungal pathogen *Fusarium oxysporum* f. sp. *cubense* (Foc). This pathogen is divided into four races based on host specificity. In the early twentieth century, Foc race 1 led to the near-complete devastation of the widely cultivated *Gros Michel* cultivar. In response, the banana industry shifted to the *Cavendish* cultivar, which displayed resistance to race 1. However, the emergence of tropical race 4 (Foc TR4), capable of infecting *Cavendish* bananas, has led to significant economic losses and poses a major challenge to global banana production [1, 2].

Foc TR4 has strong stress tolerance, capable of surviving in soil for decades and spreading through contaminated soil, water, tools, and infected plant material. Current management strategies, including chemical fungicides, breeding of resistant cultivars, and biocontrol measures, have shown limited effectiveness. This limited success is due in part to the pathogen's strong stress resistance, the poor fertility of *Cavendish* bananas, and the perennial nature of banana cultivation [2, 3]. To persist in the soil and successfully colonize host roots, Foc TR4 must not only withstand environmental stresses but also compete with or suppress resident microbial communities in the rhizosphere. Recent studies suggest that manipulating the rhizosphere microbiome, the complex community of microbes surrounding plant roots, offers a promising avenue for mitigating *Fusarium* wilt disease [4–6]. The rhizosphere microbiome, often referred to as the plant's "second genome," serves as a protective barrier against soil-borne pathogens by competing for resources and ecological spaces [7]. To establish infection, Foc TR4 must overcome these microbiome-mediated defenses. The concept of a "core microbiota" within the rhizosphere has further advanced our understanding of plant–microbe interactions. Core microbiota refers to a subset of microbial species that exert significant influence on microbiome assembly and host health. These hub species contribute to nutrient acquisition, plant growth promotion, and disease suppression [8]. Recent advances to design synthetic microbial communities or engineered microbiomes have shown promise in providing these benefits in agricultural systems [9–11]. However, their efficacy is often limited to laboratory or green house conditions, as field applications must contend with the complexity of plant-pathogen-microbe interactions [12, 13]. Therefore, understanding how soil-borne pathogens like Foc TR4 interact with and manipulate the rhizosphere microbiome is essential for developing effective and sustainable strategies to control *Fusarium* wilt disease.

Fungal secondary metabolites are increasingly recognized as key regulators in microbial interactions, playing diverse roles including protection against environmental stresses, regulation of fungal development, and serving as ecological tools for interspecies competition [14]. Historically, these compounds have been extensively studied for their significance in both medicine and agriculture. Landmark examples include aflatoxin, the poison responsible for Turkey X disease in the 1960 s, and the penicillin, the first broad-spectrum antibiotic, both of which highlight the dual nature of secondary metabolites as harmful toxins and therapeutic agents. Secondary metabolites are synthesized from primary metabolic pathways and include a wide range of chemical classes, such as polyketides, terpenes, and non-ribosomal peptides. Unlike primary metabolite genes, which are dispersed throughout the fungal genome, secondary metabolite biosynthetic genes are usually organized into contiguous clusters. This clustered arrangement enables coordinated regulation, allowing fungi to rapidly produce specific secondary metabolites in response to environmental and ecological pressures [14].

Despite extensive research into their pharmacological properties, the ecological roles of secondary metabolites in native microbial communities remain elusive. Among these compounds, fungal pigments stand out as biologically active secondary metabolites with potential applications in medicine, agriculture, and industry [15]. Pigments such as quinones, flavonoids, melanin, and azaphilones have been reported to protect fungi from environmental stresses, including ultraviolet radiation and oxidative damage [16, 17]. Additionally, many of these compounds are being explored as natural dyes and pigments. However, their roles in mediating microbial interactions, particularly within the rhizosphere, are still largely unexplored.

Bikaverin is a reddish pigment produced by several *Fusarium* species. First identified in *Fusarium fujikuroi*,

bikaverin is a polyketide metabolite that accumulates within fungal mycelia and is secreted into the surrounding medium, giving both the fungal colony and its substrate a characteristic reddish color. This compound exhibits a broad range of biological activities, including anti-protozoal effects against *Leishmania brasiliensis*, antitumoral activity against different cancer cells, inhibitory effects on rat mitochondria [18], and antimicrobial activity against several bacterial and fungal species [19]. Additionally, bikaverin shows efficacy in controlling plant pathogens, such as tomato late blight caused by *Phytophthora infestans* [20], and exhibits nematicidal activity against the pine wood nematode *Bursaphelenchus xylophilus* [21]. Despite these known bioactivities, the ecological role of bikaverin in *Fusarium* species, particularly its involvement in interactions with the rhizosphere microbiome, remains unknown.

Given the critical role of microbial interactions in shaping plant health and disease resistance, understanding how secondary metabolites like bikaverin influence these dynamics is essential. Interestingly, many antibiotics, most of which are secondary metabolites, have long been recognized as molecular tools for targeting pathogenic bacteria in humans and animals. However, their broad-spectrum activity often leads to unintended disruption of beneficial microbial communities, altering overall microbiome composition [22]. By analogy, we hypothesize that soil-borne pathogens like Foc TR4 may employ secondary metabolites to suppress or eliminate beneficial rhizosphere microbes, thereby weakening microbiome-mediated defenses and promoting infection.

In this study, we hypothesize that Foc TR4 uses bikaverin to manipulate the rhizosphere microbiome by suppressing plant growth-promoting rhizobacteria (PGPRs), which enhances its ability to infect banana roots. To test this hypothesis, we generated a bikaverin-deficient mutant strain by knocking out the gene encoding the key enzyme in the bikaverin biosynthetic pathway. We then assessed its pathogenicity and examined its effects on rhizosphere microbiome composition using 16S rRNA and ITS sequencing. Additionally, we isolated bikaverin-resistant strains to explore their potential as biocontrol agents against *Fusarium* wilt disease. Our findings reveal a novel ecological role for bikaverin in microbial community manipulation and provide a foundation for future microbiome engineering strategies aimed at banana wilt disease management.

Materials and methods

Fungal strains and culture conditions

Foc TR4 (isolate B2) was previously isolated and is maintained in our laboratory [23]. The Foc TR4 strains were cultivated on potato dextrose agar (PDA) medium or complete/minimal medium agar plates at 28 °C for 5–7 days. For liquid cultures, the strains were grown under shaking conditions at 28 °C and 160 rpm for 1–3 days.

Construction of gene knockout, complementation, and green fluorescent protein (GFP) expression mutant strains

The Foc TR4 mutant strains were constructed following previously established procedures [23, 24]. Briefly, the key gene *FocBik1*, responsible for bikaverin biosynthesis, was knocked out using a homologous recombination strategy, as illustrated in Fig. S1a. The upstream and downstream flanking regions of *FocBik1* were amplified, ligated with the Hygromycin phosphotransferase gene (*HPT*) truncated sequences, and subsequently used to replace the *FocBik1* coding sequence. Recombinant fragments comprising the truncated *FocBik1* sequence, its native promoter, and the Neomycin phosphotransferase gene (*NPTII*) were assembled. These fragments were subsequently used to replace the *HPT* sequence in the knockout mutant (Fig. S1c). To generate GFP-tagged strains, a GFP expression plasmid was utilized [24]. After that, the linearized DNA fragments were introduced into Foc TR4 protoplasts according to previous procedures [24]. Transformants were selected using 100 mg mL^{-1} G418 or 300 mg mL^{-1} Hygromycin B (Sigma-Aldrich, St Louis, MO, USA).

Gene knockout mutants were validated by two rounds of PCR analysis to confirm the correct integration of the recombinant fragments into the *FocBik1* locus. The first round used primer pairs flanking the homologous arms (Bik1-JC5 F/HPH-JC3R, HPH-JC5 F/Bik1-JC3R), the second round used primers of *FocBik1* nucleotide sequence (Bik1-OF/Bik1-OR). Complementation strains were analyzed by PCR amplification of the *FocBik1* nucleotide sequence. The verified transformants were purified via single-conidial isolation by spreading the conidial suspension onto Malt Extract Agar medium (MEA) supplemented with G418 or G418/Hygromycin. Single-conidial isolates were further confirmed through PCR analysis. The gene knockout mutant was named Δ*FocBik1*, and the complementation mutant was named as Res-Δ*FocBik1*. All primers used for gene amplification and validation are listed in Table S1.

Inoculation of banana plantlets and pathogenicity assay

Banana plantlets (*Musa acuminata* L. AAA group, "Brazilian") at five-leaf stage and approximately 90 days old were obtained from the Tissue Culture Center of Chinese Academy of Tropical Agricultural Sciences. The plantlets were maintained under greenhouse conditions following our previously established protocol [23]. For banana inoculation, each banana plantlet was irrigated

with 50 mL of conidial suspension in ddH_2O at concentration of 2×10^6 conidia mL^{-1}, making the final concentration of approximately 10^6 conidia per gram of soil. After a 5-week incubation period, the disease index was calculated based on the extent of pseudostem browning, as described in earlier studies [24]. Each treatment group consisted of 20 banana plantlets, with plantlets inoculated with ddH_2O serving as control. All plantlets were randomly assigned to treatment groups to minimize positional and handling bias. The experiment was performed in duplicate to ensure reproducibility.

Extraction and HPLC–MS analysis of bikaverin

Bikaverin was recovered from Foc TR4 cultures using liquid minimal medium supplemented with yeast extract as the nitrogen source (pH 4.0). Cultures were incubated under shaking conditions at 28 °C and 160 rpm for 3 days. Following cultivation, mycelium was removed by filtration, and conidia were separated via centrifugation at 6000 rpm for 10 min. The resulting filtrate was further clarified by passing it through a 0.45-μm cellulose acetate membrane filter. The resulting supernatant was subjected to bikaverin extraction using ethyl acetate at a 3:1 ratio (50-mL ethyl acetate per 150-mL supernatant) [25]. The mixture was vortexed rigorously and allowed to stand for phase separation. The ethyl acetate layer was collected and freeze-dried to yield a reddish crude bikaverin product. The crude bikaverin was dissolved in DMSO, and its concentration was determined using a BioTek Synergy H1 microplate reader by measuring absorbance at 500 nm [26]. Quantification was based on a calibration curve ($Abs500 = 0.0006 \times [\text{bikaverin, } \mu g\ mL^{-1}] + 0.0447$, $R^2 = 0.9999$). The bikaverin solution was then adjusted to a final concentration of 1250 μg mL^{-1} to prepare a stock solution, which was stored at − 80 °C until further used.

For high-performance liquid chromatography-mass spectrometry (HPLC–MS) analysis, the crude product from 100 mL of supernatant was dissolved in 1 mL of 80% methanol containing 0.1% formic acid, and the pH was adjusted to 5.8 using additional formic acid. The resulting solution was syringe-filtered and used for further analysis. HPLC–MS/MS analysis was carried out on an AB SCIEX Triple Quad 5500 + system platform equipped with Analyst software (Version 1.7.1) and an electrospray ionization (ESI) source. Chromatographic separation followed a binary gradient on an AB SCIEX ExionLC system as described previously [27]. The separation was performed on an AB SCIEX ExionLC system coupled with a Venusil MP C18 column (Agela, VA931002 -0). The flow rate was maintained at 300 μL min^{-1}. The mass spectrometer operated in positive ion mode. Key MS settings included an ion spray voltage of 5.5 kV, a desolvation temperature of 500 °C, a declustering potential (DP) of 50, and a collision energy (CE) of 45. The mass spectrometric fragmentation ions of m/z 340.2 $[(M^+H)^+–C_2H_3O]$ and m/z 270.3 $[(M^+H)^+–C_3H_2O_2]$, along with a retention time of 13.48 min, were used for the confirmation of bikaverin. The relative content of bikaverin was quantified using peak area ratios, as calculated with SCIEX OS 2.1.6 software.

Vegetative growth, conidiation assay, and stress tolerance

The vegetative growth of Foc TR4 strains was evaluated by culturing them on complete and minimal media, followed by measurement of colony diameter. Conidiation capacity was assessed by culturing the strains in liquid medium and quantifying conidial production. Stress tolerance was examined by exposing the strains to various chemical stressors to simulate environmental challenges. The treatments included 0.7 mol L^{-1} sodium chloride (NaCl) for osmotic stress, 1 mol L^{-1} sorbitol for hyperosmotic stress, 30 mmol L^{-1} hydrogen peroxide (H_2O_2) for oxidative stress, 10 mmol L^{-1} dithiothreitol (DTT) for redox imbalance, 0.25 mg L^{-1} Congo red for cell wall integrity stress, and 0.1 μg L^{-1} sodium dodecyl sulfate (SDS) for membrane stress. Each treatment was performed in triplicate, and all experiments were independently repeated twice for reproducibility. Conidiation capacity was also evaluated.

Microscopic analysis of Foc TR4 infection in banana roots

To investigate the infection and colonization of Foc TR4 strains in banana root vascular, tissue-cultured banana seedlings were employed. The roots of the seedlings were inoculated by immersing them in a conidial suspension at a concentration of 10^6 conidia mL^{-1} for 30 min. Following inoculation, the seedlings were transferred to 1/2 Murashige and Skoog (MS) medium and cultured for 1 week under controlled conditions. After the incubation period, the roots were rinsed thoroughly with sterile water and carefully sliced into sections approximately 0.5–1 mm in thickness. The sections were stained with propidium iodide (PI) for 10 min to enhance visualization of cellular structures. Stained root sections were then observed under a Leica DM6000 microscope, and images were captured for further analysis. Microscopic images were analyzed using ImageJ software (http://rsbweb.nih.gov/ij/, v. 1.47 g).

RT-qPCR analysis

To investigate gene expression responses to pH conditions, Foc TR4 strains were cultured in liquid minimal medium at pH of 4.0, 7.0, and 9.0, respectively. After 2 days of incubation, mycelia were harvested for RNA isolation, with the mycelia cultured at pH 4.0 serving as the reference sample. For dual-culture experiments, Foc

TR4 strains were co-cultured with other microbes on minimal medium agar plates for 5 days. Mycelia from the contact edge of the colonies were collected for RNA isolation, and mycelia from Foc TR4 WT strains cultured alone were used as the reference sample. The total RNA isolation, first-strand cDNA synthesis, and qPCR analysis were carried out as described previously [28]. Total RNA was extracted using the RNAprep Pure Plant Plus Kit (TIANGEN Biotech, Beijing, China), and first-strand cDNA was synthesized with FastKing gDNA Dispelling RT SuperMix (TIANGEN Biotech, Beijing, China). Quantitative PCR (qPCR) analysis was performed using ChamQ SYBR Color qPCR Master Mix (Vazyme, Nanjing, China) on a QuantStudio 6 system (Thermo Fisher, Waltham, MA, USA). The relative transcript levels of target genes were calculated using the $2^{-\Delta\Delta Ct}$ method [29], with *FocActin* serving as the endogenous control [23]. Each reaction involved three biological replicates.

Bikaverin's inhibitory effect assay

To evaluate the inhibitory effects of bikaverin on various microbes, crude bikaverin extract prepared as described above was utilized for treatment assays. For bacterial growth assay, two bacterial strains isolated from soil, *Bacillus velezensis* and Actinomycetes strain DMS16689, were used to assess bikaverin's antibacterial activity. The bacteria were cultured in liquid Luria–Bertani (LB) medium supplemented with crude extracts from both Foc TR4 WT and bikaverin-deficient mutant (Δ*FocBik1*) strains. Bacterial growth was monitored over time by measuring optical density at 600 nm (OD600), and growth curves were generated to analyze the effects of bikaverin. To assess the antifungal activity of bikaverin, two plant fungal pathogens, *Colletotrichum gloeosporioides* and *Botrytis cinerea*, were employed. Crude bikaverin extract was incorporated into PDA medium. The colony growth of the fungal pathogens was recorded and analyzed to determine the inhibitory effects of bikaverin on fungal growth.

Pathogenicity assay under sterile conditions

To eliminate the influence of the natural microbiome, the pathogenicity of Foc TR4 WT and Δ*FocBik1* strains was evaluated under sterile conditions using tissue-cultured banana seedlings. Roots of the banana seedlings were gently rinsed with sterile water to remove surface contaminants. The seedlings were then immersed in a conidia suspension (10^6 conidia mL^{-1}) from either WT or Δ*FocBik1* strains for 30 min. Control seedlings were treated with sterile distilled water (ddH_2O). Following inoculation, a group of seedlings was transferred into individual sterile jars containing fresh 1/2 MS medium. Then the seedlings were cultured at 25 °C under a 16-h light/8-h dark photoperiod. After 3 weeks, the disease symptoms of the seedlings were recorded. At the same time, the other group of inoculated seedlings was transplanted into sterile pots containing autoclaved soil. The pots were maintained in greenhouse environment. After 4 weeks, disease symptoms of the seedlings were evaluated based on visible leaf yellowing.

Rhizosphere soil sampling

Natural soil was collected from a healthy banana plantation field and mixed with autoclaved nutrient soil at a 1:1 ratio to serve as the growth medium for banana seedlings. Banana seedlings at the five-leaf stage were transplanted into pots containing this soil mixture and cultured for 2 weeks to establish root systems. After 2 weeks, the soil was inoculated with Foc TR4 conidia suspension. To prevent rapid fungal growth, the conidia suspension concentration was adjusted to 2×10^3 conidia mL^{-1}. Each seedling received 50 mL of the conidia suspension, resulting in a final concentration of approximately 10^3 conidia per gram of soil. Control samples were treated with ddH_2O under identical conditions and were included in all experimental setups to ensure consistent baseline comparisons. After 3 weeks of incubation, rhizosphere soil was collected following previously described methods [4, 30]. Briefly, fresh roots of three healthy plants per plot were pooled into a composite rhizosphere soil sample. After loose soil was slightly shaken off the root surface, the composite root sample were washed with sterile saline solution to remove tightly adhering soil particles. The saline solution containing soil particles was centrifuged at 6000 $\times g$ for 6 min, and the resulting precipitate was collected. After that, the rhizosphere soil samples were stored at −80 °C for further DNA extraction. A total of six rhizosphere soils were prepared for each treatment.

DNA extraction and amplification sequencing

Total DNA was extracted from collected rhizosphere soil samples using the HiPure Soil DNA Kit (Magen, Guangzhou, China) following the manufacturer's instructions. Amplification and sequencing were performed by Gene Denovo Biotechnology (Guangzhou, China). The 16S rDNA region of the ribosomal RNA (rRNA) gene for bacteria and the ITS sequence for fungi were amplified using primers listed in Table S1. PCR products were evaluated on 2% agarose gels, and amplicons were purified using AMPure XP Beads (Beckman, CA, USA) as per the manufacturer's protocol. Libraries were prepared using the Illumina DNA Prep Kit (Illumina, CA, USA) and assessed for quality using an ABI StepOnePlus Real-Time PCR System (Life Technologies, Foster City, USA). Paired-end

sequencing (2 × 250 bp reads) was performed on the Illumina Novaseq 6000 platform.

The raw reads obtained were processed and filtered using FASTP (version 0.18.0) [31]. Paired reads were subsequently merged into raw tags using FLASH (version 1.2.11) [32]. Sequences with ≥ 97% similarity were clustered into operational taxonomic units (OTUs) using the UPARSE pipeline (version 9.2.64) [33], while chimeric sequences were identified and removed with the UCHIME algorithm [34]. The tag sequence with the highest abundance within each OTU cluster was selected as the representative sequence for further analysis. Raw sequences were analyzed using QIIME 2 on the CentOS 7.6 environment [35]. Taxonomic classifications of OTUs were assigned using the SILVA database (version 138) for bacterial sequences and the UNITE database (version 7.2) for fungal sequences. Additionally, representative OTU or amplicon sequence variant (ASV) sequences were classified into taxa using the naive Bayesian model implemented in the RDP Classifier (version 2.2) [36], with a confidence threshold of 0.8. Alpha diversity analysis was calculated in QIIME (version 1.9.1) [37]. Beta diversity metrics were computed and visualized using the Vegan package in R [38]. Principal coordinates analysis (PCoA) was employed to assess differences in microbial community composition. Group comparisons were conducted using Tukey's HSD test and the Kruskal–Wallis H test, implemented in the Vegan package in R (version 2.5.3). Statistical significance was set at $P < 0.05$.

Isolation of bikaverin resistant bacteria

To isolate bikaverin-resistant bacteria, rhizosphere soil samples were collected from banana plants grown in a Foc TR4-inoculated plots. Approximately 1 g of rhizosphere soil was suspended in 10 mL of sterile saline, vortexed for 10 min, and then serially diluted to 10^{-6} in sterile saline. LB agar plates were prepared with increasing concentrations of crude bikaverin extract at 5‰, 10‰, 25‰, and 50‰, corresponding to final concentrations of 6.25, 12.5, 31.25, and 62.5 μg mL^{-1}, respectively, to systematically narrow the selection range for resistant bacteria. A 100 μL aliquot from each dilution was spread onto the agar plates and incubated at 28 °C for 48–72 h. Colonies capable of growing on bikaverin-supplemented plates were considered potential bikaverin-resistant isolates. After completing four rounds of selection, the resistance of the isolated strains to bikaverin was further validated by culturing them in liquid LB medium supplemented with bikaverin at 5‰ and 10‰. Bacterial growth dynamics were monitored by measuring the OD600 every 3 h for a 24-h period.

To assess their potential as biocontrol agents, the antifungal activity of the bikaverin-resistant bacteria was tested against Foc TR4. Antagonistic assays were performed on potato dextrose agar (PDA) plates using the dual-culture method. A bacterial suspension (5 μL) was dropped 3 cm away from fungal colonies, and the plates were incubated at 28 °C for 5 days. Growth inhibition zones around the bacterial colonies were measured to evaluate their antagonistic effect on Foc TR4.

Statistical analyses

All experiments were conducted with at least three biological replicates, and the data were expressed as mean ± standard deviation (SD). Statistical analyses were performed using R software (version 4.2.2) and SPSS Statistics (version 27.0, IBM, USA) as mentioned above. Statistical significance was set at $P < 0.05$.

Results

Bikaverin is not required for vegetative growth but plays a role in pathogenicity of Foc TR4

The genome analysis of Foc TR4 revealed a conserved gene cluster responsible for bikaverin biosynthesis (Fig. 1a). This cluster comprises six genes: *FocBik1* (FOIG_14908), encoding a typical type I

(See figure on next page.)

Fig. 1 Role of bikaverin in the vegetative growth and pathogenicity of *Fusarium oxysporum* f. sp. *cubense* TR4 (Foc TR4). **a** Schematic representation of the bikaverin biosynthetic gene cluster in the wild-type (WT) and the *FocBik1* knockout mutant (Δ*FocBik1*). *FocBik1*, encoding a polyketide synthase, was replaced with a neomycin phosphotransferase II (*NPTII*) cassette in Δ*FocBik1*. **b** Quantification of bikaverin production in WT, Δ*FocBik1*, and uninoculated control cultures by LC–MS. Bars represent mean peak areas of bikaverin-specific ions. Δ*FocBik1* exhibits no detectable bikaverin production. Data are presented as mean ± standard deviations. **c** Colony morphology of WT, Δ*FocBik1*, and complemented strain (Res-Δ*FocBik1*) on complete medium (CM), minimal medium (MM), and under various abiotic stress conditions. **d** Colony diameter of WT, Δ*FocBik1*, and Res-Δ*FocBik1* after 7 days of growth on CM and MM. **e** Quantification of conidiation of WT, Δ*FocBik1*, and Res-Δ*FocBik1* cultured in liquid complete medium. **f** Growth inhibition of WT, Δ*FocBik1*, and Res-Δ*FocBik1* under abiotic stress conditions. Data are presented as mean ± standard deviations. Letters indicate statistical significance determined by one-way ANOVA with Duncan's multiple range test ($P < 0.05$). **g** Disease symptom and index of banana plantlets inoculated with WT, Δ*FocBik1*, and Res-Δ*FocBik1*. Representative images of pseudo-stem browning are shown, with the corresponding disease index distribution across plantlets. **h** Infection and colonization of banana roots by GFP-tagged strains of WT and Δ*FocBik1* visualized after 7 days of inoculation. Bright-field (BF), GFP fluorescence, propidium iodide (PI) staining, and merged images are presented. Arrows indicate vascular colonization by WT

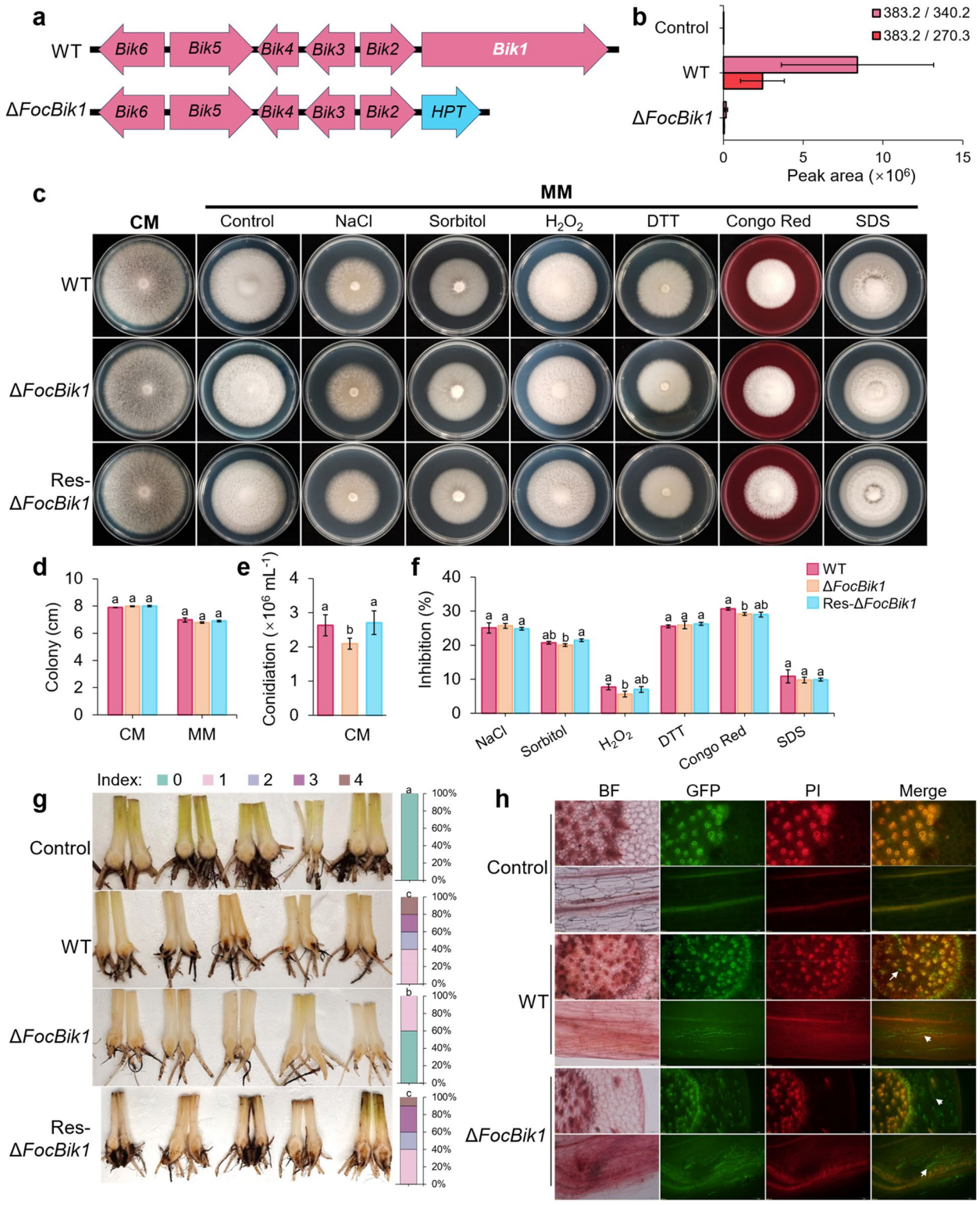

Fig. 1 (See legend on previous page.)

fungal polyketide synthase (PKS); *FocBik2* (FOIG_14907), encoding a putative FAD-dependent monooxygenase; *FocBik3* (FOIG_14906), encoding an O-methyltransferase; *FocBik4* (FOIG_14905), encoding a transcription factor enhancer; *FocBik5* (FOIG_14904), encoding a transcription factor regulating cluster expression; and *FocBik6* (FOIG_14903), encoding a bikaverin efflux pump. Among these, FocBik1 catalyzes the initial and rate-limiting step of bikaverin production, converting precursors into prebikaverin.

To elucidate the biological roles of bikaverin, a *FocBik1* knockout mutant (Δ*FocBik1*) was generated via a homologous recombination strategy (Fig. S1a, b). The complementation strain was constructed by introducing the expression cassette into the genome of the knockout mutant (Fig. S1c, d). When cultured on minimal medium agar supplemented with yeast extract as a nitrogen source, the Foc TR4 wild-type strain (WT) displayed a pale reddish pigmentation, whereas the Δ*FocBik1* strain exhibited a complete absence of red pigmentation (Fig. S1e). To quantify bikaverin production, Foc TR4 strains were cultured in liquid minimal medium for 2 days, after which mycelia were collected and intracellular bikaverin levels measured via LC–MS. The results indicated that Δ*FocBik1* produced negligible amounts of bikaverin (Fig. 1b; Fig. S2). These findings confirm that the deletion of *FocBik1* effectively abolishes bikaverin production in Foc TR4. Thus, the Δ*FocBik1* strain was used as a bikaverin-deficient mutant for subsequent studies.

The effects of bikaverin on vegetative growth, conidiation, and abiotic stress tolerance were subsequently investigated. The results revealed that bikaverin deficiency did not impact vegetative growth but slightly reduced the conidiation of Foc TR4 (Fig. 1c–e). Additionally, bikaverin had an overall minimal effect on abiotic stress tolerance, although Δ*FocBik1* exhibited slightly increased sensitivity under osmotic (sorbitol), oxidative (H_2O_2), and cell wall (Congo red) stress conditions (Fig. 1c, f). These findings suggest that bikaverin is not essential for vegetative growth or stress tolerance in Foc TR4.

To assess the role of bikaverin in pathogenicity, conidial suspensions of the mutant strains were inoculated into banana plantlet roots. After 4 weeks, pseudo-stem browning was scored to determine the disease index. The results (Fig. 1g) showed that the WT strain caused disease in 40% of plantlets at index 1 and 20% at index 2, 3, and 4, respectively, resulting in an average disease index of 2.2. In contrast, 60% of plantlets inoculated with Δ*FocBik1* displayed no disease symptoms, while the remaining plantlets were limited to index 1, with no disease scores exceeding index 2. And the average disease index for Δ*FocBik1*-treated plantlets was only 0.6.

To assess whether bikaverin is required for infection and colonization of plant roots, GFP-tagged strains were used to infect banana tissue culture seedlings. After 7 days of inoculation, microscopic examination of root sections showed that both the WT and Δ*FocBik1* strains successfully infected and colonized the vascular bundles (Fig. 1h). These results suggest that while bikaverin contributes to the overall pathogenicity of Foc TR4, it is not essential for root infection.

Bikaverin production is induced by acidic conditions and biological competition

To determine whether bikaverin production is influenced by environmental pH, Foc TR4 strains were cultured in minimal medium supplemented with yeast extract (YE) as a nitrogen source at varying pH levels. The results revealed that at pH 4, the WT strain produced abundant bikaverin, evident from the reddish coloration of the culture broth. In contrast, when cultured at pH 7 and pH 9, bikaverin production was markedly reduced, as indicated by the absence of red pigmentation in the broth (Fig. 2a). These findings suggest that acidic conditions can induce bikaverin production. Additionally, in contrast to the organic nitrogen source YE, the inorganic nitrogen source $NaNO_3$ failed to induce bikaverin biosynthesis. To investigate whether the increased bikaverin production under acidic conditions was due to the induction of biosynthetic genes, the relative expression levels of *FocBik1* were analyzed. The results corroborated the observed bikaverin production patterns: cultures grown in YE at pH 4 exhibited significantly elevated transcription of *FocBik1*, with about sevenfold up-regulation; while neutral, alkaline conditions (pH 7 and pH 9) or $NaNO_3$ as a nitrogen source did not induce gene expression (Fig. 2b).

To explore whether competition with other microbes could induce bikaverin production, three common plant and soil microorganisms, *B. cinerea*, *B. velezensis*, and *Actinomycetes* strain DMS16689, were co-cultured with Foc TR4 in dual culture assays. The results demonstrated that dual culture with *B. cinerea* led to visible reddish pigmentation at the contact margin between the two colonies (Fig. 2c); In contrast, co-culture with the bacteria *B. velezensis* or *Actinomycetes* resulted in slight red pigment production across the entire Foc TR4 colony. To validate the induction of bikaverin biosynthetic genes during microbial competition, the colony margins were collected and analyzed via RT-qPCR. The results revealed that the relative expression level of *FocBik1* was significantly upregulated under all competitive conditions (Fig. 2d). Taken together, these findings suggest that, in addition to organic nitrogen sources and acidic environmental conditions, biological competition also serves as a key inducer of bikaverin production.

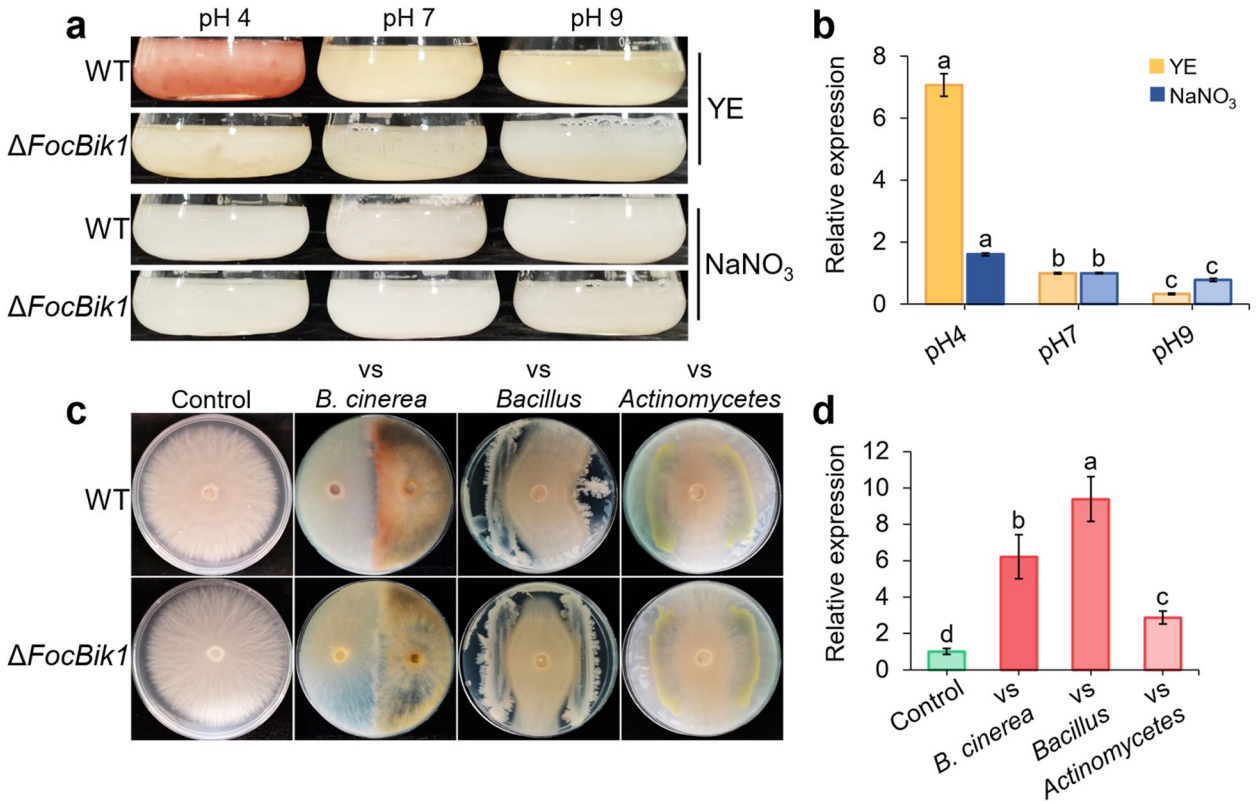

Fig. 2 Environmental and biological factors induce bikaverin production in *Fusarium oxysporum* f. sp. *cubense* TR4 (Foc TR4). **a** Bikaverin production by wild-type (WT) and *FocBik1* knockout mutant (Δ*FocBik1*) strains cultured in minimal medium with yeast extract (YE) or sodium nitrate ($NaNO_3$) as the nitrogen source under different pH conditions (pH 4, pH 7, and pH 9). **b** Relative expression levels of *FocBik1* in WT strains grown in YE or $NaNO_3$ at pH 4, 7, and 9. The mycelium cultured at pH 7 was used as the reference samples. Data are presented as mean ± standard deviations. Letters indicate statistical significance determined by one-way ANOVA with Duncan's multiple range test ($P < 0.05$). **c** Dual culture assays of WT and Δ*FocBik1* strains with *Botrytis cinerea*, *Bacillus velezensis*, and *Actinomycetes* strain DMS16689. **d** Relative expression levels of *FocBik1* in WT strains during dual culture with *B. cinerea*, *B. velezensis*, and *Actinomycetes*. Data are presented as mean ± standard deviations. Letters indicate statistical significance determined by one-way ANOVA with Duncan's multiple range test ($P < 0.05$)

Bikaverin acts as an antimicrobial agent against soil bacteria and fungi

Since microbial competition was observed to induce the production of bikaverin, we hypothesized that bikaverin might function as an "antibiotic" by inhibiting the growth of competing microbes. To validate this hypothesis, we tested the sensitivity of two bacterial species (*B. velezensis* and *Actinomycetes* strain DMS16689) and two fungal pathogens (*C. gloeosporioides* and *B. cinerea*) to extracts derived from *Foc* TR4 culture broth. Bikaverin was firstly extracted from the Foc TR4 broth using ethyl acetate, air-dried, and dissolved in DMSO (Fig. 3a).

The inhibitory effects of the extracts on microbial growth were subsequently assessed by measuring growth curves for the bacteria and colony diameters for the fungi. For *B. velezensis*, the results demonstrated a dose-dependent inhibitory effect: 1‰ WT extract (corresponding to 1.25 μg mL^{-1} bikaverin) reduced bacterial growth, while 2‰ WT extract (corresponding to 2.5 μg mL^{-1} bikaverin) completely inhibited growth (Fig. 3b, c). For *Actinomycetes*, the 2‰ WT extract was lethal to bacterial growth, while the 1‰ WT extract showed mild inhibitory effects. In contrast, the Δ*FocBik1* extract exhibited no impact on bacterial growth, suggesting that the inhibitory effect is specifically mediated by bikaverin. These findings indicate that bikaverin exerts potent antimicrobial activity, with varying degrees of efficacy depending on the concentration and target species. For the fungal pathogens, *C. gloeosporioides* showed no significant growth inhibition under either the WT or Δ*FocBik1* extract treatments. However, the 2‰ WT extract effectively repressed the growth of *B. cinerea*, suggesting that bikaverin selectively targets certain fungal species (Fig. 3d, e). Importantly, neither the WT nor Δ*FocBik1* extracts impacted the growth of Foc TR4 itself, indicating that bikaverin does not exhibit self-toxicity under these experimental

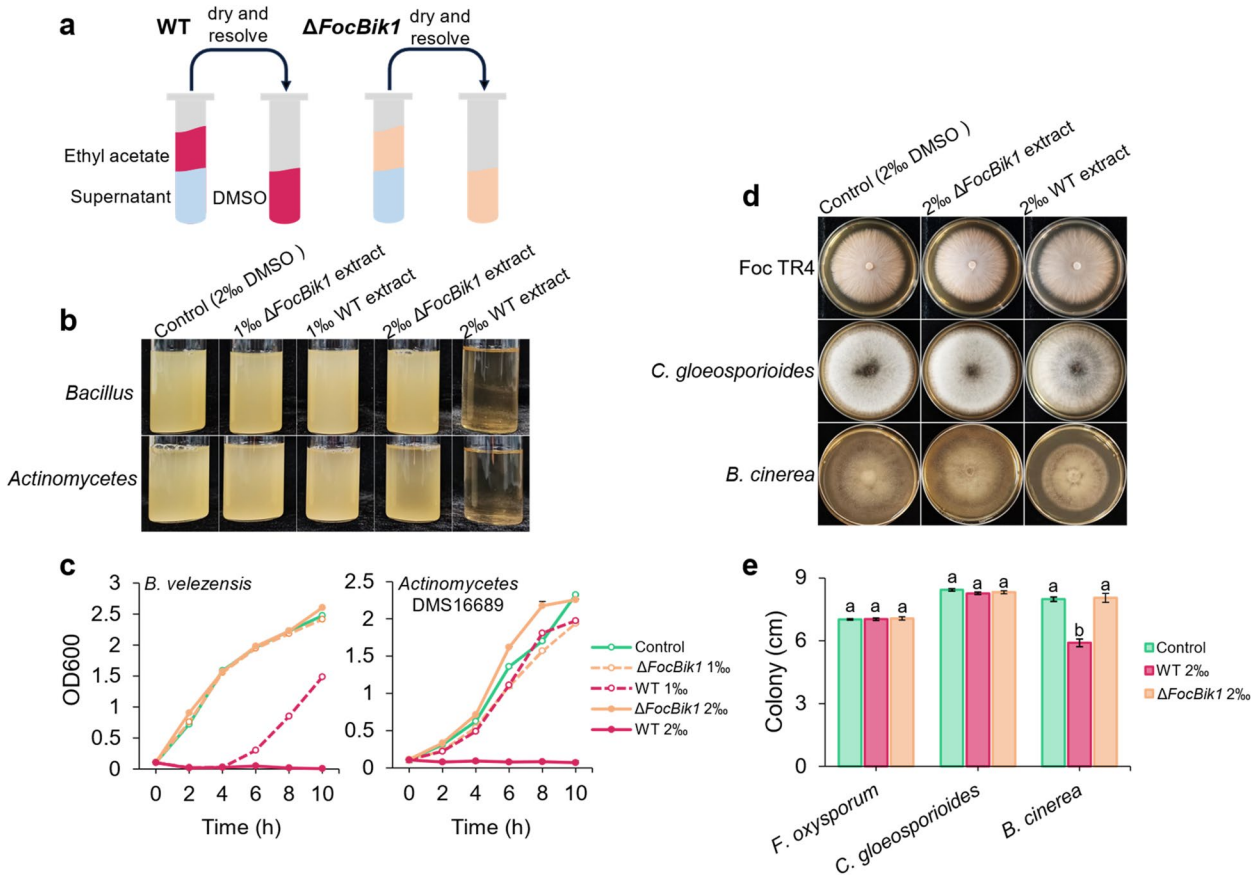

Fig. 3 Antimicrobial activity of bikaverin extracted from *Fusarium oxysporum* f. sp. *cubense* TR4 (Foc TR4). **a** Schematic representation of bikaverin extraction from wild-type (WT) and *FocBik1* knockout mutant (Δ*FocBik1*) cultures. **b** Inhibitory effects of WT and Δ*FocBik1* extracts on *Bacillus velezensis* and *Actinomycetes* strain DMS16689. Bacterial growth was monitored in the presence of 1‰ and 2‰ WT or Δ*FocBik1* extracts. The 1‰ and 2‰ WT extracts corresponded to 1.25 and 2.5 μg mL.$^{-1}$ bikaverin, respectively. **c** Growth curves of *B. velezensis* and *Actinomycetes* strain DMS16689 in the presence of WT and Δ*FocBik1* extracts. Data are presented as mean ± standard deviations. **d** Colony growth of Foc TR4, *Colletotrichum gloeosporioides*, and *Botrytis cinerea* on agar plates supplemented with WT and Δ*FocBik1* extracts. **e** Quantification of colony diameters for fungal growth under different treatments. Data are presented as mean ± standard deviations. Letters indicate statistical significance determined by one-way ANOVA with Duncan's multiple range test ($P < 0.05$)

conditions. Taken together, these findings demonstrate that bikaverin functions as an effective antimicrobial agent, capable of suppressing the growth of certain bacteria and fungi during microbial competition, highlighting bikaverin's potential ecological role as a competitive advantage for Foc TR4 in soil environments.

Bikaverin indirectly regulates the pathogenicity of Foc TR4

To evaluate whether bikaverin directly regulate pathogenicity of Foc TR4, a series of experiments were conducted under controlled conditions without natural microbiome interference. Tissue culture banana seedlings were inoculated with WT or Δ*FocBik1*, and pathogenicity was evaluated under both sterile and autoclaved soil conditions (Fig. 4a). In the first experimental setup, inoculated seedlings were transferred to a sterile growth medium, creating an environment devoid of external microbial influences. Disease progression was assessed over several weeks. The results demonstrated no significant difference in plant disease symptoms, suggesting that bikaverin does not directly contribute to the pathogenicity of Foc TR4 in the absence of microbial interactions (Fig. 4b). In the second setup, inoculated seedlings were transplanted into autoclaved soil, where limited interactions with the native microbiome could occur. Consistent with the results observed in sterile medium, there were no significant differences in disease severity between WT and Δ*FocBik1*-treated plants (Fig. 4c). Both strains exhibited comparable levels of disease severity, further supporting the conclusion that bikaverin is not directly involved in Foc TR4's pathogenicity when microbial competition is excluded.

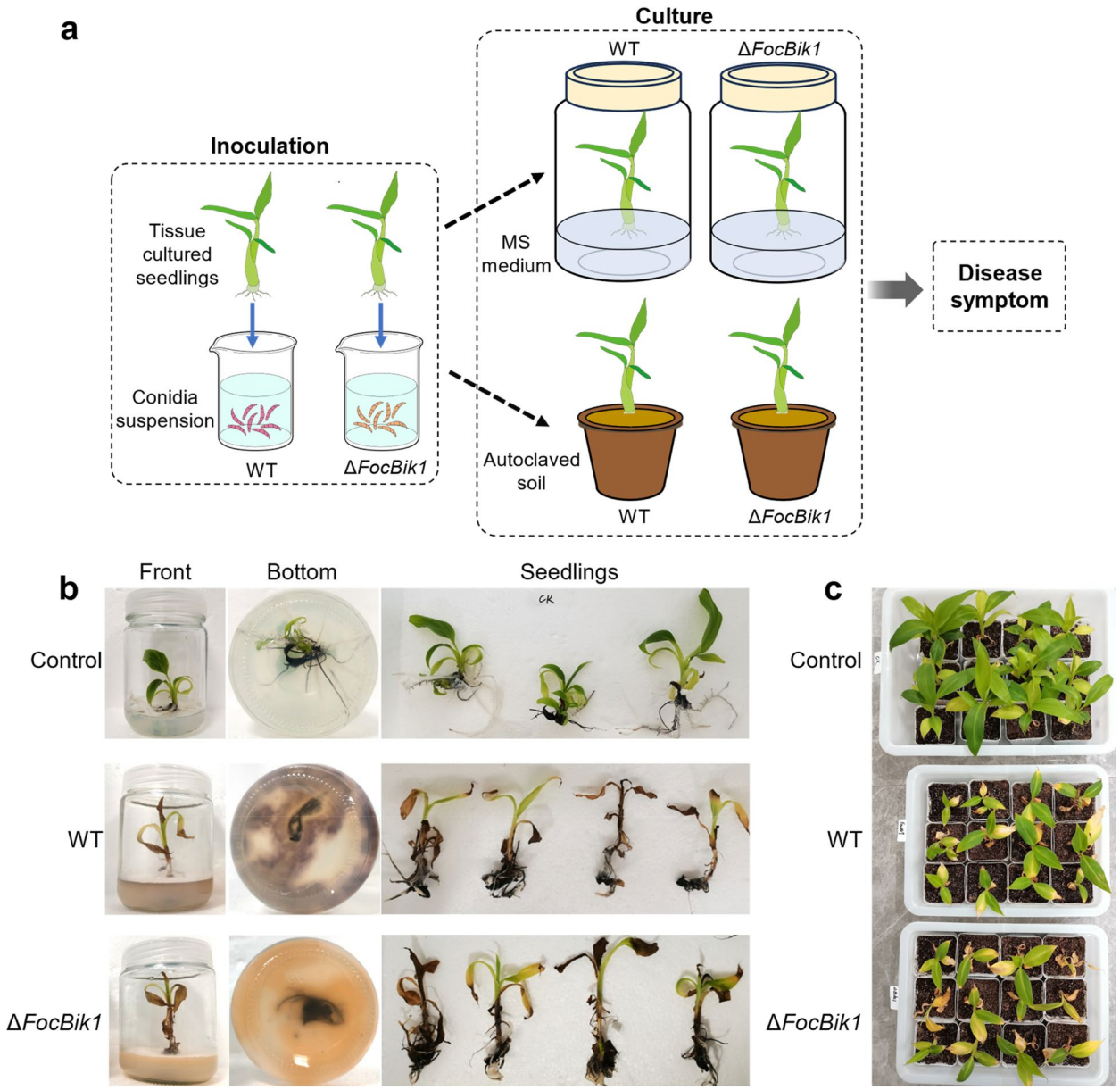

Fig. 4 Bikaverin does not directly regulate the pathogenicity of Foc TR4 under sterile conditions. **a** Experimental design for evaluating the pathogenicity of wild-type (WT) and bikaverin-deficient mutant (Δ*FocBik1*) strains in tissue-cultured banana seedlings. Seedlings were inoculated with conidial suspensions of WT or Δ*FocBik1* and grown either in sterile Murashige and Skoog (MS) medium or autoclaved soil. **b** Disease symptoms of banana seedlings grown in sterile MS medium. **c** Disease symptoms of banana seedlings grown in autoclaved soil

Impact of bikaverin on rhizosphere microbiome composition

To investigate the role of bikaverin in shaping rhizosphere microbial communities, Banana plants were treated with Foc TR4 WT and Δ*FocBik1* strains, respectively, and left uninoculated as a control (CK). 16S rRNA sequencing was employed to profile bacterial communities, and ITS sequencing was used to characterize fungal communities. For 16S rRNA sequencing, we obtained an average of 100,216, 98,578, and 101,631 effective tags for CK, WT, and Δ*FocBik1* samples, respectively. For ITS sequencing, the corresponding averages were 121,772, 119,829, and 122,867 tags. Rarefaction curve analysis (Fig. S3) showed that all samples reached a plateau, indicating that the sequencing depth was sufficient to capture the majority

of microbial diversity in both bacterial and fungal communities.

For bacterial community, principal coordinate analysis (PCoA) revealed distinct clustering of rhizosphere microbial communities among the three treatments, indicating that WT and Δ*FocBik1* significantly altered the microbiome composition compared to CK. PCo1 and PCo2 explained 42.28% and 7.71% of the variance, respectively, demonstrating that the WT strain had a stronger impact on microbiome structure than the bikaverin-deficient mutant (Fig. 5a). Alpha diversity metrics further highlighted the effect of bikaverin on microbial communities. The WT-inoculated rhizosphere exhibited slightly higher ACE and Shannon diversity indices compared to CK and Δ*FocBik1* treatments (Fig. 5b). This indicates that WT treatment enhances rhizosphere microbial diversity, whereas the absence of bikaverin production in Δ*FocBik1* limits its influence on community structure. Taxonomic profiling revealed substantial shifts in microbial composition at the phylum, family, and genus levels (Table S2–4). At the phylum level, WT treatment caused a significant reduction in Firmicutes compared to CK, while Δ*FocBik1* increased the relative abundance of Firmicutes. Both WT and Δ*FocBik1* treatments increased the relative abundance of *Bacteroidota* and *Acidobacteriota* compared to CK (Fig. 5c). At the genus level, WT treatment significantly reduced the abundance of *Bacillus* and *Paenibacillus*, well-known PGPRs, while increasing the relative abundance of genera such as *Bryobacter*, *Bauldia*, *SM1 A02P*, and other unclassified taxa. In contrast, Δ*FocBik1*-treated rhizospheres exhibited an increase in *Bacillus* abundance, with *Paenibacillus* showing a slight decrease compared to CK (Fig. 5c). These results suggested that *Bacillus*, one of the most abundant genera in rhizosphere microbial communities, is a primary target of bikaverin.

ITS sequencing revealed that fungal communities in the rhizosphere were also significantly affected by WT and Δ*FocBik1* treatments (Table S5–7). PCoA demonstrated distinct clustering of fungal communities among the three treatments, with WT and Δ*FocBik1* exerting different effects on fungal composition compared to CK. PCo1 and PCo2 explained 59.16% and 31.53% of the variance, respectively (Fig. 5d). Alpha diversity metrics further highlighted the influence of bikaverin on fungal communities. The ACE index was significantly higher in *ΔFocBik1*-treated samples compared to CK, suggesting an increase in fungal species richness. Meanwhile, the Shannon diversity index was significantly higher in WT-treated samples, indicating that WT treatment enhanced fungal diversity to a greater extent than Δ*FocBik1* (Fig. 5e). Taxonomic profiling at the family level revealed that both WT and Δ*FocBik1* treatments decreased the relative abundance of *Entolomataceae*, *Helotiaceae*, and *Chaetomiaceae*. Conversely, both treatments increased the relative abundance of *Wallemiaceae*, with Δ*FocBik1* showing a more pronounced effect than WT. At the genus level, both treatments increased the abundance of *Wallemia* and *Fusarium*, but the WT treatment resulted in significantly higher *Fusarium* abundance compared to Δ*FocBik1* (Fig. 5f). This suggests that bikaverin enhances the colonization potential of *Fusarium* in the rhizosphere, which may be a key strategy for further Foc TR4 pathogenicity.

Overall, these findings demonstrate that bikaverin plays a critical role in reshaping the rhizosphere microbiome by modulating both bacterial and fungal communities. By selectively suppressing PGPRs such as *Bacillus* and modulating fungal taxa *Fusarium*, bikaverin acts as a molecular weapon for Foc TR4, enabling it to manipulate rhizosphere microbial dynamics in its favor during colonization and infection.

Isolation of bikaverin resistant bacteria with biological control potential

Building on the above findings, we hypothesized that isolating or engineering bikaverin-resistant microbes, particularly bacteria, could provide potential biological control agents for combating banana wilt disease. To test this hypothesis, rhizosphere bacteria were isolated from banana seedlings inoculated with the Foc TR4 WT strain for 3 weeks. The isolation process employed agar medium supplemented with Foc TR4 extracts as a selective pressure. After 4 rounds of isolation, during which the concentration of the Foc TR4 extract was incrementally increased, seven strains exhibiting high resistance to bikaverin were identified (Fig. S4). The bikaverin resistance of these isolates was further analyzed in liquid culture. Three bikaverin-sensitive strains were selected as negative controls. The results (Fig. 6a) demonstrated that 10‰ WT extract effectively suppressed the growth of most bacteria. In contrast, the Δ*FocBik1* extract had minimal impact on bacterial growth, except for strain R91, which exhibited growth inhibition during the early culture stages. Among the resistant strains, R131, R158, and R160 displayed the highest resistance to bikaverin, with R160 demonstrating exceptional recovery, as its growth resumed within 9 h of culture.

To evaluate the biological control potential of these isolates, their ability to inhibit Foc TR4 was assessed in vitro. *B. velezensis*, known for its high biological control efficacy in vitro based on previous studies, was used as a positive control. Comparison of colony area reduction revealed that four strains, R128, R131, and R160, exhibited high control effects, reducing the Foc TR4 colony area by over 50% (Fig. 6b, c).

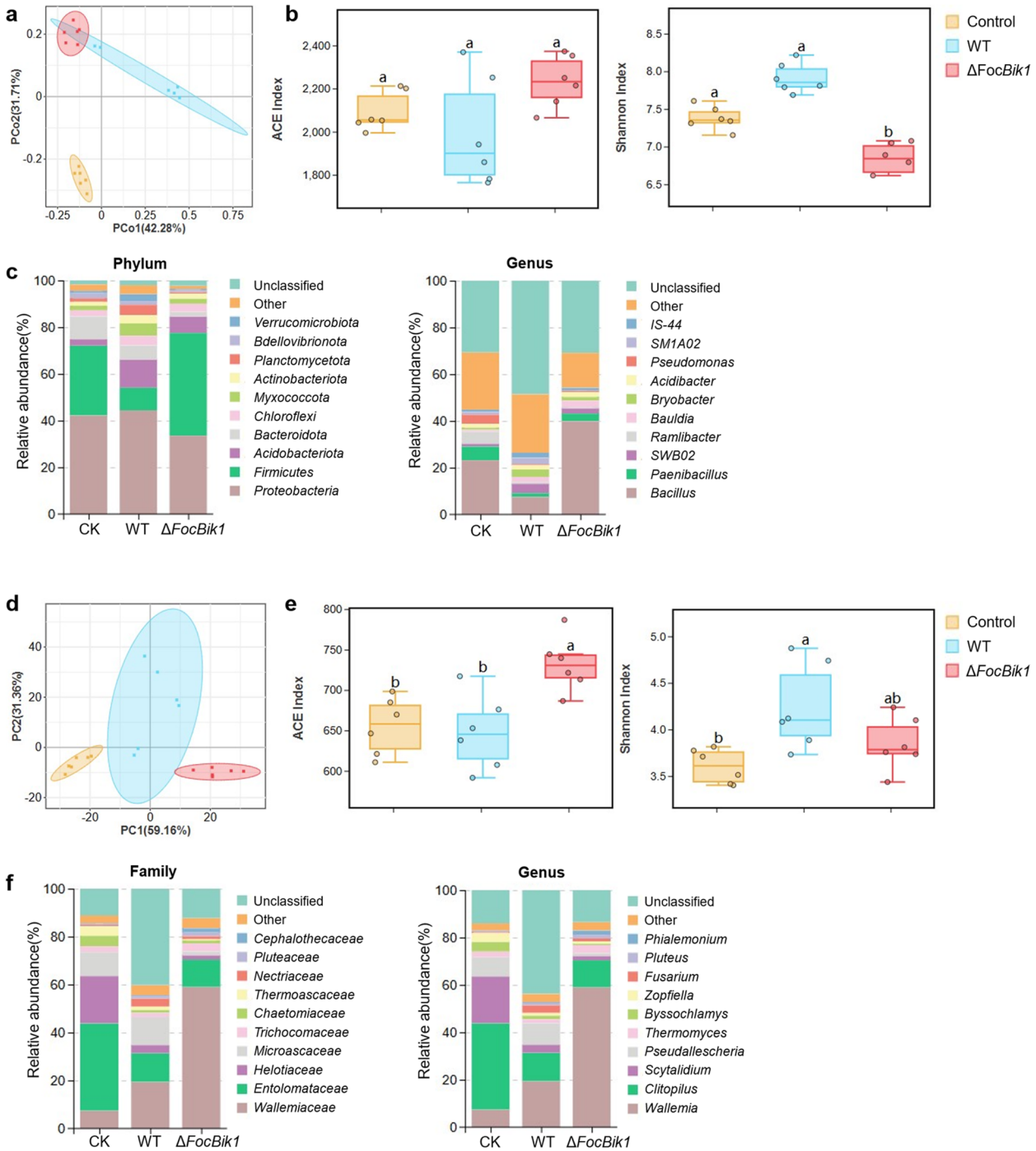

Fig. 5 Bikaverin reshapes the bacterial and fungal communities in the rhizosphere of banana plants. **a** Principal coordinate analysis (PCoA) of bacterial community composition in the rhizosphere of uninoculated control (CK), wild-type (WT), and bikaverin-deficient mutant (Δ*FocBik1*) treatments based on 16S rRNA sequencing. **b** Alpha diversity indices (ACE and Shannon) of bacterial communities. Data are presented as mean ± standard deviations (n = 6 biologically independent replicates). Letters indicate statistical significance ($P < 0.05$). **c** Taxonomic profiles of bacterial communities at the phylum and genus levels, showing the top 12 most abundant taxa. **d** PCoA of fungal community composition in the rhizosphere based on ITS sequencing. **e** Alpha diversity indices (ACE and Shannon) of fungal communities. Data are presented as mean ± standard deviations (n = 6 biologically independent replicates). Letters indicate statistical significance ($P < 0.05$). **f** Taxonomic profiles of fungal communities at the family and genus levels, showing the top 12 most abundant taxa

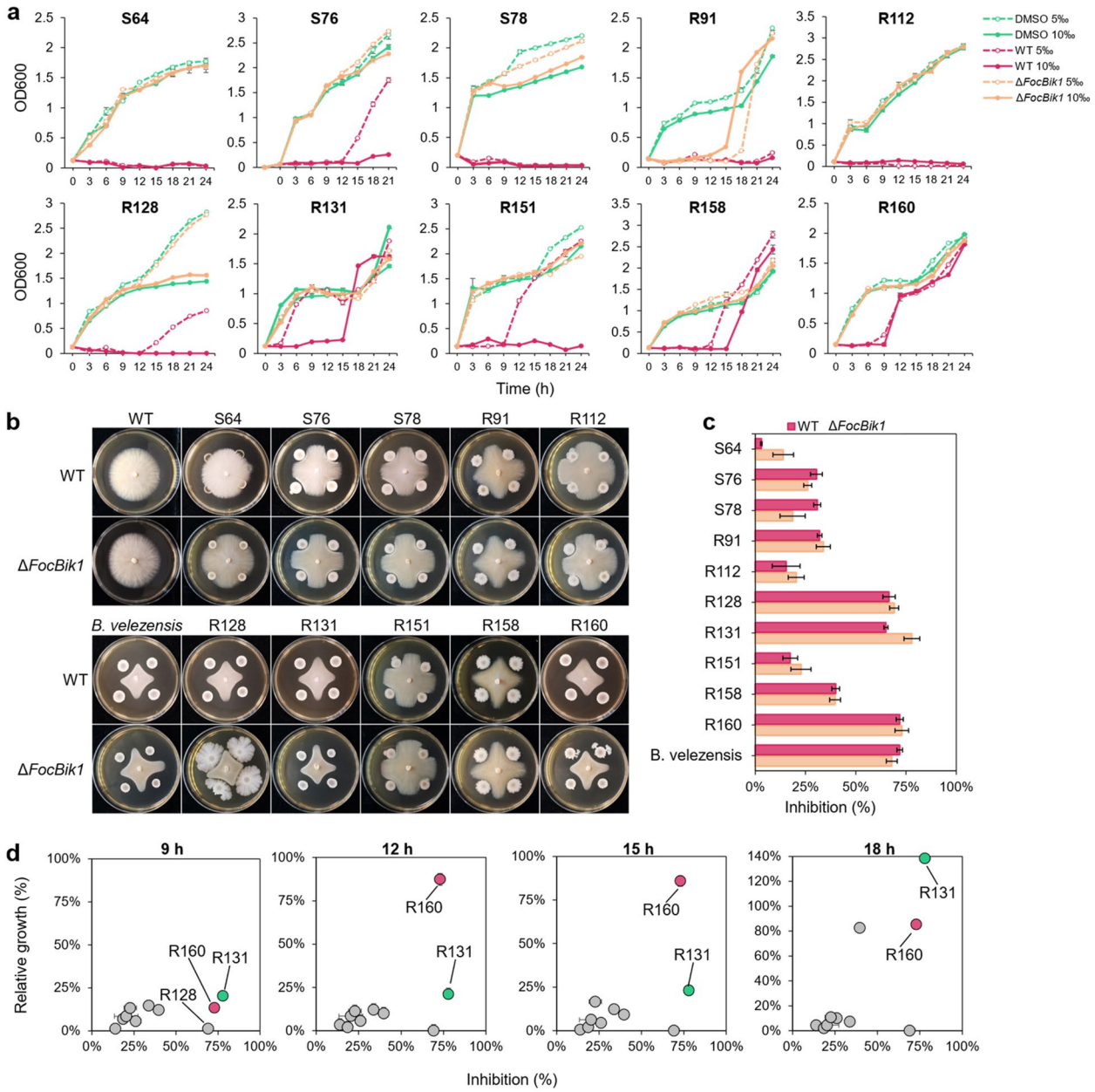

Fig. 6 Isolation and characterization of bikaverin-resistant bacteria with biological control potential. **a** Growth curves of bacterial isolates, S64, S76, S78, R91, R112, R128, R131, R151, R158, and R160, in liquid medium supplemented with 5‰ and 10‰ extracts from WT or Δ*FocBik1* cultures. The 5‰ and 10‰ WT extracts corresponded to 6.25 and 12.5 μg $mL.^{-1}$ bikaverin, respectively. **b** In vitro inhibition of Foc TR4 by bacterial isolates. Foc TR4 was co-cultured with bacterial strains on agar plates. **c** Quantification of inhibition percentages for Foc TR4 colony growth in co-culture experiments. Data are presented as mean ± standard deviations**. d** Scatter plots of relative growth under bikaverin treatment versus inhibition percentages of Foc TR4 by bacterial isolates at 9, 12, 15, and 18 h. The red spot indicates strain R160, and the green one indicates strain R131

An integrative analysis of bikaverin resistance and biological control efficacy was performed to identify strains with the best dual performance. Relative growth under bikaverin treatment was calculated for each strain at different time points using the formula: Relative growth (%) = (OD600 of treated sample/OD600 of control sample) × 100%. A scatter plot of the data (Fig. 6d) revealed that R160 displayed the best combination of bikaverin resistance and biological control effect. Strain R131 also demonstrated strong potential, though its overall performance was slightly less than R160. In contrast, while R158 displayed a high biological control effect against Foc

TR4, it exhibited relatively high sensitivity to bikaverin, limiting its utility as a robust candidate. In addition, to investigate whether strain R160 could raise the pH of the medium and thereby create a hostile environment for bikaverin production, we incubated the strain for 2 days and monitored pH changes. The results (Fig. S5) showed that R160 actually lowered the pH of the medium rather than increasing it, suggesting that its effectiveness appears to stem from resistance to bikaverin. These results suggest that R160 support R160 as a promising biocontrol agent against Foc TR4, combining high pathogen suppression efficacy with bikaverin resistance.

R160 identified as a bacillus strain with broad spectrum biological control potential

To identify strain R160, 16S rRNA DNA was amplified and sequenced. The results confirmed that R160 belongs to the *Bacillus* genus (Fig. S6a). To further resolve its species, the housekeeping gene *gyrA* was amplified and sequenced. However, the sequence did not match any known strain with 100% identity in the NCBI database (Fig. S6b). As a result, the strain was designated *Bacillus* BR160. To evaluate the biological potential of *Bacillus* BR160, its inhibitory effects on several fungal pathogens were tested in vitro. The results demonstrated that *Bacillus* BR160 exhibited strong antifungal activity against multiple pathogens, including *Fusarium oxysporum f. sp. lycopersici*, *Fusarium falciforme*, *C. gloeosporioides*, and *B. cinerea*, highlighting its broad-spectrum biological control capabilities (Fig. S7). These findings suggest that *Bacillus* BR160 holds significant promise as a biological control agent for combating fungal diseases, including *Fusarium* wilt.

Discussion

Fungal secondary metabolites represent a diverse group of bioactive compounds crucial for survival, ecological competition, and interaction with other organisms. These compounds are products of secondary metabolic pathways that exhibit remarkable structural and functional diversity. Among these, polyketides represent a group of secondary metabolites with pharmaceutical, agricultural, and industrial significance due to their wide-spectrum biological activities, including antimicrobial, anticancer, and antifungal uses [39, 40]. Bikaverin is a red-colored tetracyclic polyketide with antibacterial and anticancer activities [18, 20, 41, 42], and this compound has been found unique to several members of *Fusarium* species till now [43, 44]. While prior research has predominantly focused on bikaverin's medical applications and biosynthetic pathways [45], its ecological and functional roles, particularly in the context of *Fusarium* pathogenicity and rhizosphere interactions—remain underexplored.

Fusarium species are well-known for producing a diverse array of secondary metabolites, many of which play significant roles in ecological adaptation and pathogenicity. Nofigexamples include gibberellins, phytohormones involved in plant growth modulation, and other metabolites like fusaric acid, beauvericin, and moniliformin, which further demonstrate the metabolic diversity of these fungi [14]. Among these, metabolites like fusaric acid are recognized for their direct pathogenic strategies. Fusaric acid is a classic example of a virulence factor with a direct role in disease progression. Previous studies have shown that fusaric acid disrupts potassium homeostasis and induces reactive oxygen species accumulation in host cells, thereby compromising cellular defenses and enhancing susceptibility to infection [46]. In contrast, our findings reveal that bikaverin operates through a fundamentally different mechanism. Pathogenicity assays conducted under sterile and autoclaved conditions, where microbial interactions were minimized, demonstrated no significant differences in disease severity between WT and bikaverin-deficient mutant strains of Foc TR4. Additionally, in vitro assays confirmed that bikaverin exhibits antimicrobial activity against both soil bacteria and fungi (Fig. 3). These results suggest that bikaverin's role in pathogenicity is indirect, mediated through ecological rather than physiological processes. Instead, the following studies demonstrated that bikaverin enhances Foc TR4 pathogenicity indirectly by reshaping the rhizosphere microbiome.

The rhizosphere microbiome plays a central role in plant health, influencing nutrient acquisition, stress resistance, and disease suppression [8, 47, 48]. Beneficial microbes within the rhizosphere, particularly PGPRs, enhance plant health by producing phytohormones, solubilizing nutrients, and secreting antimicrobial compounds [49, 50]. Our findings demonstrate that bikaverin functions as a molecular weapon, enabling *Fusarium oxysporum* to disrupt the rhizosphere microbiome and gain a competitive advantage. Specifically, WT strain significantly reduced the abundance of *Bacillus* and *Paenibacillus*, key plant growth-promoting rhizobacteria [51]. Simultaneously, it promoted the proliferation of fungal genera such as *Fusarium* and *Trichocladium*. This disruption of the rhizosphere microbiome undermines the natural defense mechanisms of plants and provides a competitive advantage to the pathogen. In addition, bikaverin-deficient mutant also influenced the rhizosphere microbial community, although to a lesser extent than WT. Foc TR4 is known to produce other secondary metabolites such as fusaric acid, which may also contribute to microbiome modulation. Fusaric acid has been reported to exert antimicrobial effects and may influence microbial community structure indirectly by

altering host root exudates [52]. These findings suggest that bikaverin plays a pivotal role in microbial manipulation, while other secondary metabolites may act synergistically or independently to further influence rhizosphere dynamics.

Furthermore, our study extends prior insights into bikaverin biosynthesis by elucidating its regulation under environmental conditions. Acidic pH and nitrogen were found to significantly induce bikaverin production in Foc TR4, consistent with earlier studies showing that bikaverin biosynthesis is highly responsive to environmental stimuli. For example, previous research has demonstrated that nitrogen starvation and low pH enhance mRNA levels of bikaverin biosynthetic genes [18, 41, 53]. Additionally, sulfate and phosphate starvation further stimulate bikaverin biosynthesis, indicating a multifaceted regulation involving nutrient scarcity. Sucrose also serves as a specific positive signal for bikaverin production, potentially regulated at the post-transcriptional level [54]. Notably, our findings reveal a novel regulatory mechanism for bikaverin biosynthesis—its induction through microbial competition. During dual-culture experiments, bikaverin production was significantly elevated in response to interactions with competing microbes, such as *B. cinerea*. This highlights microbial competition as a potent ecological trigger for bikaverin biosynthesis, supporting its role as a competitive molecular tool under resource-limited environments. This highlights microbial competition as a potent ecological trigger for bikaverin biosynthesis, supporting its role as a competitive molecular tool under resource-limited environments. Similar patterns of metabolite-mediated cross-regulation have been observed in fungal interactions, where secondary metabolites such as polyketides and terpenes function in attack–counterattack strategies [55]. These observations suggest that bikaverin may be part of a broader chemical dialogue among soil microbes. Additionally, in animal cells, bikaverin has been shown to disrupt mitochondrial membrane structure at relatively high concentrations, while at lower concentrations, it suppresses NAD- and succinate-related respiration without directly affecting the electron transport chain [56]. However, the mechanism underlying its antimicrobial activity in microbes remains unclear. Further studies are needed to elucidate how bikaverin exerts toxicity against bacterial and fungal targets.

As plant growth-promoting rhizobacteria, *Bacillus* species are vital for plant health, promoting growth and systemic resistance through the production of antifungal lipopeptides like surfactin and iturin [50, 57–59]. The suppression of *Bacillus* by bikaverin has critical implications for plant health. Bikaverin's ability to inhibit these beneficial microbes allows *F. oxysporum* to colonize plant roots more effectively by undermining the plant's natural microbial defenses. Moreover, our study highlights bikaverin's role in promoting fungal dominance. Fungal taxa, such as *Trichocladium*, were enriched in bikaverin-treated rhizospheres, suggesting that bikaverin not only suppresses bacterial competitors but also adjusts conditions favorable to fungal growth. Similar phenomenon has been reported for some other metabolites. For example, gliotoxin, a secondary metabolite produced by several fungi, including *Trichoderma virens*, not only acts as an immunosuppressant in hosts but also exhibits antimicrobial activity, inhibiting bacterial competitors and thereby promoting fungal colonization within microbial communities [60, 61]. Moreover, while bikaverin has been shown to reshape the rhizosphere microbiome and suppress beneficial bacteria such as *Bacillus*, similar microbial manipulation mechanisms have been observed with fungal effectors, which target host immunity and promote fungal colonization [62].

The identification of bacteria capable of resisting various environmental stresses could significantly enhance their application in agriculture and improve plant growth under adverse conditions. For instance, chromium-resistant bacteria have been demonstrated to reduce chromium toxicity in soils, improving microbial activity and crop productivity through bioremediation strategies [63, 64]. Similarly, aluminum-resistant microbes such as *Rhodococcus erythropolis* and *Pseudomonas aeruginosa* have been shown to confer aluminum tolerance to plants by mitigating soil acidification and enhancing nutrient availability in acidic soils [65, 66]. Selenium-tolerant bacteria not only survive in selenium-rich environments but also transform toxic selenium compounds into bioavailable forms, thereby improving plant growth and selenium uptake for nutritional benefits [67].

These results inspired us with the concept that the identification of bikaverin-resistant microbes might offer a novel strategy for counteracting *F. oxysporum* in pathogen-affected soils. Beneficial microbes that can withstand bikaverin's antimicrobial effects are likely to thrive in *Fusarium*-dominated rhizospheres and suppress pathogen proliferation. Then we set up to isolate bikaverin resistant strains. The strain *Bacillus* BR160 was identified with high bikaverin resistance, moreover, this strain showed a broad-spectrum antifungal activity against fungal pathogens, including *B. cinerea*, *C. gloeosporioides*, and *Fusarium* species, making it a robust candidate for integrated pest management strategies.

Taken together, this study highlights the multifaceted role of bikaverin as a secondary metabolite in Foc TR4. While bikaverin does not directly contribute to pathogenicity under sterile conditions, it significantly influences disease progression by reshaping the

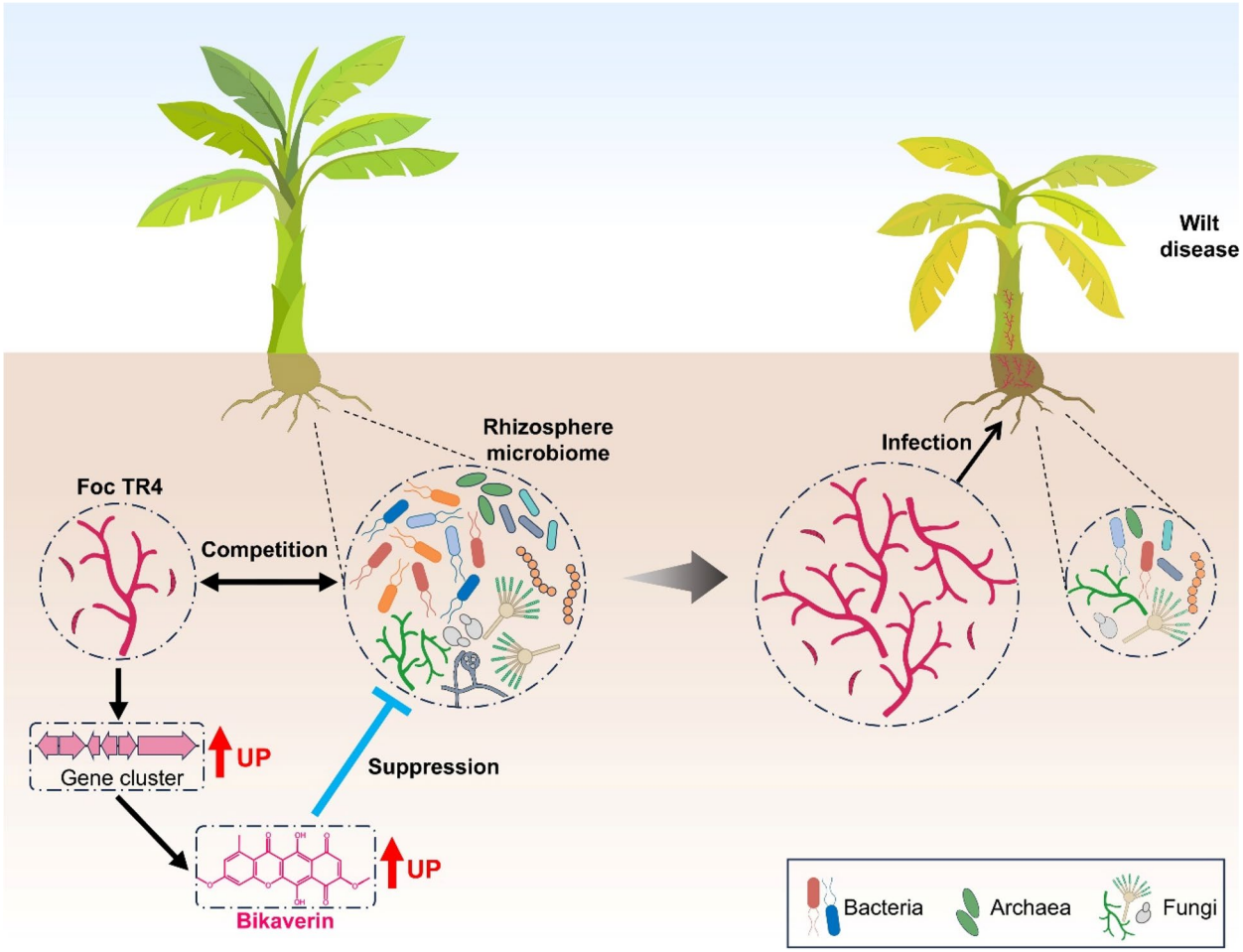

Fig. 7 The schematic illustrates the functional role of bikaverin in *Fusarium oxysporum* f. sp. *cubense* TR4 (Foc TR4) during banana wilt disease progression. During competition with other rhizosphere microbes, bikaverin biosynthesis is upregulated, suppressing key PGPRs such as *Bacillus* spp. The resulting disruption of the microbial community gives Foc TR4 a competitive advantage, facilitating root colonization and infection, ultimately leading to wilt symptoms in banana plants

rhizosphere microbiome. By suppressing beneficial PGPRs like *Bacillus* and promoting fungal dominance, bikaverin establishes a microbial environment favorable for *Fusarium* colonization and infection (Fig. 7). The identification of bikaverin-resistant microbes, particularly *Bacillus* BR160, offers promising avenues for biocontrol strategies against banana wilt disease. In the Future research, omics-based approaches are needed to unravel the molecular pathways targeted by bikaverin and elucidate resistance mechanisms in *Bacillus* BR160. Additionally, efforts should focus on engineering microbial consortia that integrate *Bacillus* BR160 with other plant growth-promoting rhizobacteria to enhance disease resistance.

Supplementary Information

The online version contains supplementary material available at https://doi.org/10.1186/s40168-025-02109-7.

Additional file 1: Supplementary data revised

Additional file 2: Supplementary tables

Acknowledgements

We thank Dr. Chunming Dong from Third Institute of Oceanography, Ministry of Natural Resources of China for kindly donation of Actinomycetes strain DMS16689.

Authors' contributions

Bang An and Qiannan Wang: conceived and designed the study. Honglin Lu, Suxia Guo, Yongbao Yang, Zhihao Zhao, Qingbiao Xie, Changjun Sun, Bang An performed the experiments and analyzed the data. Qiong Wu and Hongli Luo: funding acquisition and project administration. Honglin Lu, Bang An and Qiannan Wang wrote the manuscript. All authors commented on and approved the final manuscript.

Funding

The study was financially supported by the National Natural Science Foundation of China (32001846, 32260042, 32160594), the Key Research and Development Project of Hainan Province (ZDYF2024XDNY214), and the Project of Sanya Yazhou Bay Science and Technology City (SCKJ-JYRC- 2024–15).

Data availability
The datasets generated for the current study are available for the public. All data including bacteria and fungi from amplicon sequencing was deposited at The National Center for Biotechnology Information (NCBI) with the accession number PRJNA1197142.

Declarations

Ethics approval and consent to participate
Not applicable.

Consent for publication
Not applicable.

Competing interests
The authors declare no competing interests.

Author details
[1]National Key Laboratory for Tropical Crop Breeding, School of Breeding and Multiplication (Sanya Institute of Breeding and Multiplication), School of Tropical Agriculture and Forestry (School of Agriculture and Rural Affairs & School of Rural Revitalization), Hainan University, Sanya, Hainan Province, People's Republic of China. [2]Key Laboratory of Banana Genetic Improvement of Hainan Province, Institute of Tropical Bioscience and Biotechnology, Chinese Academy of Tropical Agricultural Sciences, Haikou, Hainan Province 571101, People's Republic of China.

Received: 13 December 2024 Accepted: 9 April 2025
Published online: 29 April 2025

References

1. Ploetz RC. Panama disease: an old nemesis rears its ugly head: part 1. The beginnings of the banana export trades. Plant Health Prog. 2005;6(1):18.
2. Ordonez N, Seidl MF, Waalwijk C, Drenth A, Kilian A, Thomma BPHJ, et al. Worse comes to worst: bananas and panama disease—when plant and pathogen clones meet. PLoS Pathog. 2015;11(11): e1005197.
3. Ismaila AA, Ahmad K, Siddique Y, Wahab MAA, Kutawa AB, Abdullahi A, et al. *Fusarium* wilt of banana: current update and sustainable disease control using classical and essential oils approaches. Hortic Plant J. 2023;9(1):1–28.
4. Fu L, Penton CR, Ruan Y, Shen Z, Xue C, Li R, Shen Q. Inducing the rhizosphere microbiome by biofertilizer application to suppress banana *Fusarium* wilt disease. Soil Biol Biochem. 2017;104:39–48.
5. Zhou D, Jing T, Chen Y, Wang F, Qi D, Feng R, et al. Deciphering microbial diversity associated with *Fusarium* wilt-diseased and disease-free banana rhizosphere soil. BMC Microbiol. 2019;19(1):161.
6. Qiu M, Zhang R, Xue C, Zhang S, Li S, Zhang N, Shen Q. Application of bio-organic fertilizer can control *Fusarium* wilt of cucumber plants by regulating microbial community of rhizosphere soil. Biol Fertil Soils. 2012;48:807–16.
7. Berendsen RL, Pieterse CMJ, Bakker PAHM. The rhizosphere microbiome and plant health. Trends Plant Sci. 2012;17(8):478–86.
8. Trivedi P, Leach JE, Tringe SG, Sa T, Singh BK. Plant–microbiome interactions: from community assembly to plant health. Nat Rev Microbiol. 2020;18(11):607–21.
9. Li Z, Bai X, Jiao S, Li Y, Li P, Yang Y, et al. A simplified synthetic community rescues *Astragalus mongholicus* from root rot disease by activating plant-induced systemic resistance. Microbiome. 2021;9(1):217.
10. Ruan Z, Chen K, Cao W, Meng L, Yang B, Xu M, et al. Engineering natural microbiomes toward enhanced bioremediation by microbiome modeling. Nat Commun. 2024;15(1):4694.
11. Compant S, Cassan F, Kostić T, Johnson L, Brader G, Trognitz F, et al. Harnessing the plant microbiome for sustainable crop production. Nat Rev Microbiol. 2025;23(1):9–23.
12. Hong S, Yuan X, Yang J, Yang Y, Jv H, Li R, et al. Selection of rhizosphere communities of diverse rotation crops reveals unique core microbiome associated with reduced banana *Fusarium* wilt disease. New Phytol. 2023;238(5):2194–209.
13. Liu Y, Zhu A, Tan H, Cao L, Zhang R. Engineering banana endosphere microbiome to improve *Fusarium* wilt resistance in banana. Microbiome. 2019;7(1):74.
14. Keller NP. Fungal secondary metabolism: regulation, function and drug discovery. Nat Rev Microbiol. 2019;17(3):167–80.
15. Narsing Rao MP, Xiao M, Li W. Fungal and bacterial pigments: secondary metabolites with wide applications. Front Microbiol. 2017;8:1113.
16. Medentsev AG, Arinbasarova AY, Akimenko VK. Biosynthesis of naphthoquinone pigments by fungi of the genus *Fusarium*. Appl Biochem Microbiol. 2005;41:503–7.
17. Cordero RJ, Casadevall A. Functions of fungal melanin beyond virulence. Fungal Biol Rev. 2017;31(2):99–112.
18. Limón MC, Rodríguez-Ortiz R, Avalos J. Bikaverin production and applications. Appl Microbiol Biotechnol. 2010;87(1):21–9.
19. Deshmukh R, Mathew A, Purohit HJ. Characterization of antibacterial activity of bikaverin from *Fusarium* sp. HKF15. J Biosci Bioeng. 2014;117(4):443–8.
20. Son SW, Kim HY, Choi GJ, Lim HK, Jang KS, Lee SO, et al. Bikaverin and fusaric acid from *Fusarium oxysporum* show antioomycete activity against *Phytophthora infestans*. J Appl Microbiol. 2008;104(3):692–8.
21. Kwon HR, Son SW, Han HR, Choi GJ, Jang KS, Choi YH, et al. Nematicidal activity of bikaverin and fusaric acid isolated from *Fusarium oxysporum* against pine wood nematode. Bursaphelenchus xylophilus The Plant Pathology Journal. 2007;23(4):318–21.
22. Fishbein SRS, Mahmud B, Dantas G. Antibiotic perturbations to the gut microbiome. Nat Rev Microbiol. 2023;21(12):772–88.
23. An B, Hou X, Guo Y, Zhao S, Luo H, He C, et al. The effector SIX8 is required for virulence of *Fusarium oxysporum* f. sp. *cubense* tropical race 4 to *Cavendish* banana. Fungal Biol. 2019;123(5):423–30.
24. Yang Y, An B, Guo Y, Luo H, He C, Wang Q. A novel effector, FSE1, regulates the pathogenicity of *Fusarium oxysporum* f. sp. *cubense* tropical race 4 to banana by targeting the MYB transcription factor MaEFM-like. J Fungi (Basel). 2023;9(4):472.
25. Mendonça M, Santos MCD, Pereira AK, Fill TP, Forte MBS, Bicas JL. Recovery and purification of bikaverin produced by *Fusarium oxysporum* CCT7620. Food Chemistry: X. 2021;12: 100136.
26. Santos MCD, de Lima MM, Bicas JL. Modeling bikaverin production by *Fusarium oxysporum* CCT7620 in shake flask cultures. Bioresour Bioprocess. 2020;7(1):13.
27. Arndt B, Studt L, Wiemann P, Osmanov H, Kleigrewe K, Köhler J, et al. Genetic engineering, high resolution mass spectrometry and nuclear magnetic resonance spectroscopy elucidate the bikaverin biosynthetic pathway in *Fusarium fujikuroi*. Fungal Genet Biol. 2015;84:26–36.
28. Liu S, Wang Q, Liu N, Luo H, He C, An B. The histone deacetylase HOS2 controls pathogenicity through regulation of melanin biosynthesis and appressorium formation in *Colletotrichum gloeosporioides*. Phytopathol Res. 2022;4(1):21.
29. Livak KJ, Schmittgen TD. Analysis of relative gene expression data using real-time quantitative PCR and the $2^{-\Delta\Delta CT}$ method. Methods. 2001;25(4):402–8.
30. Barillot CDC, Sarde C, Bert V, Tarnaud E, Cochet N. A standardized method for the sampling of rhizosphere and rhizoplan soil bacteria associated to a herbaceous root system. Ann Microbiol. 2013;63(2):471–6.
31. Chen S, Zhou Y, Chen Y, Gu J. fastp: an ultra-fast all-in-one FASTQ preprocessor. Bioinformatics. 2018;34(17):i884–90.
32. Magoč T, Salzberg SL. FLASH: fast length adjustment of short reads to improve genome assemblies. Bioinformatics. 2011;27(21):2957–63.
33. Edgar RC. UPARSE: highly accurate OTU sequences from microbial amplicon reads. Nat Methods. 2013;10(10):996–8.
34. Edgar RC, Haas BJ, Clemente JC, Quince C, Knight R. UCHIME improves sensitivity and speed of chimera detection. Bioinformatics. 2011;27(16):2194–200.
35. Toju H, Tanabe AS, Yamamoto S, Sato H. High-coverage ITS primers for the DNA-based identification of ascomycetes and basidiomycetes in environmental samples. PLoS ONE. 2012;7(7): e40863.
36. Wang Q, Garrity GM, Tiedje JM, Cole JR. Naive Bayesian classifier for rapid assignment of rRNA sequences into the new bacterial taxonomy. Appl Environ Microbiol. 2007;73(16):5261–7.
37. Caporaso JG, Kuczynski J, Stombaugh J, Bittinger K, Bushman FD, Costello EK, et al. QIIME allows analysis of high-throughput community sequencing data. Nat Methods. 2010;7(5):335–6.

38. Oksanen J, Blanchet FG, Friendly M, Kindt R, Legendre P, Mcglinn D, et al. Vegan: community ecology package. Ordination methods, diversity analysis and other functions for community and vegetation ecologists. Version 2.3–1. 2015. Available at: https://cran.r-project.org/package=vegan.
39. Stocker-Wörgötter E. Metabolic diversity of lichen-forming ascomycetous fungi: culturing, polyketide and shikimate metabolite production, and PKS genes. Nat Prod Rep. 2008;25(1):188–200.
40. Bills GF, Gloer JB. Biologically active secondary metabolites from the fungi. Microbiol Spectr. 2016;4(6). https://doi.org/10.1128/microbiolspec.funk-0009-2016.
41. Wiemann P, Willmann A, Straeten M, Kleigrewe K, Beyer M, Humpf HU, et al. Biosynthesis of the red pigment bikaverin in *Fusarium fujikuroi*: genes, their function and regulation. Mol Microbiol. 2009;72(4):931–46.
42. Haidar S, Aichele D, Birus R, Hielscher J, Laitinen T, Poso A, et al. In vitro and in silico evaluation of bikaverin as a potent inhibitor of human protein kinase CK2. Molecules. 2019;24(7):1380.
43. Studt L, Tudzynski B. Gibberellins and the red pigments bikaverin and fusarubin. In: Martín, JF., García-Estrada, C., Zeilinger, S. (eds) Biosynthesis and molecular genetics of fungal secondary metabolites. Fungal Biology. Springer, New York, NY. 2014;209–238.
44. Chelkowski J, Zajkowski P, Visconti A. Bikaverin production by *Fusarium* species. Mycotoxin Res. 1992;8:73–6.
45. Zhao M, Zhao Y, Yao M, Iqbal H, Hu Q, Liu H, et al. Pathway engineering in yeast for synthesizing the complex polyketide bikaverin. Nat Commun. 2020;11(1):6197.
46. Liu S, Li J, Zhang Y, Liu N, Viljoen A, Mostert D, et al. Fusaric acid instigates the invasion of banana by *Fusarium oxysporum* f. sp. *cubense* TR4. New Phytol. 2020;225(2):913–29.
47. Philippot L, Raaijmakers JM, Lemanceau P, Van Der Putten WH. Going back to the roots: the microbial ecology of the rhizosphere. Nat Rev Microbiol. 2013;11(11):789–99.
48. Yue H, Sun X, Wang T, Zhang A, Han D, Wei G, et al. Host genotype-specific rhizosphere fungus enhances drought resistance in wheat. Microbiome. 2024;12(1):44.
49. Rabbee MF, Ali MS, Choi J, Hwang BS, Jeong SC, Baek K. *Bacillus velezensis*: a valuable member of bioactive molecules within plant microbiomes. Molecules. 2019;24(6):1046.
50. Haas D, Défago G. Biological control of soil-borne pathogens by fluorescent pseudomonads. Nat Rev Microbiol. 2005;3(4):307–19.
51. Govindasamy V, Senthilkumar M, Magheshwaran V, Kumar U, Bose P, Sharma V, et al. *Bacillus* and *Paenibacillus* spp.: potential PGPR for sustainable agriculture. In: Maheshwari, D. (eds) Plant growth and health promoting bacteria. Microbiology Monographs. Springer, Berlin, Heidelberg. 2010;18:333–364.
52. Jin X, Jia H, Ran L, Wu F, Liu J, Schlaeppi K, et al. Fusaric acid mediates the assembly of disease-suppressive rhizosphere microbiota via induced shifts in plant root exudates. Nat Commun. 2024;15(1):5125.
53. Lale GJ, Gadre RV. Production of bikaverin by a *Fusarium fujikuroi* mutant in submerged cultures. AMB Express. 2016;6(1):34.
54. Rodríguez-Ortiz R, Mehta BJ, Avalos J, Limón MC. Stimulation of bikaverin production by sucrose and by salt starvation in *Fusarium fujikuroi*. Appl Microbiol Biotechnol. 2010;85(6):1991–2000.
55. Malmierca MG, Izquierdo-Bueno I, Mccormick SP, Cardoza RE, Alexander NJ, Barua J, et al. Trichothecenes and aspinolides produced by *Trichoderma arundinaceum* regulate expression of *Botrytis cinerea* genes involved in virulence and growth. Environ Microbiol. 2016;18(11):3991–4004.
56. Suzuki T, Kitagawa A, Kawai K, Hamasaki T. Reexamination of respiration-impairing effect of bikaverin on isolated mitochondria. Mycotoxin Res. 1998;14(1):19–27.
57. Alcaraz LD, Moreno-Hagelsieb G, Eguiarte LE, Souza V, Herrera-Estrella L, Olmedo G. Understanding the evolutionary relationships and major traits of *Bacillus* through comparative genomics. BMC Genomics. 2010;11:332.
58. Lugtenberg B, Kamilova F. Plant-growth-promoting rhizobacteria. Annu Rev Microbiol. 2009;63(1):541–56.
59. Xia X, Wei Q, Wu H, Chen X, Xiao C, Ye Y, et al. *Bacillus* species are core microbiota of resistant maize cultivars that induce host metabolic defense against corn stalk rot. Microbiome. 2024;12(1):156.
60. Zaid R, Koren R, Kligun E, Gupta R, Leibman-Markus M, Mukherjee PK, et al. Gliotoxin, an immunosuppressive fungal metabolite, primes plant immunity: evidence from *Trichoderma virens*-tomato interaction. mBio. 2022;13(4):e0038922.
61. Teslya AV, Gurina EV, Poshvina DV, Stepanov AA, Iashnikov AV, Vasilchenko AS. Fungal secondary metabolite gliotoxin enhances enzymatic activity in soils by reshaping their microbiome. Rhizosphere. 2024;32: 100960.
62. Snelders NC, Rovenich H, Petti GC, Rocafort M, van den Berg GCM, Vorholt JA, et al. Microbiome manipulation by a soil-borne fungal plant pathogen using effector proteins. Nat Plants. 2020;6(11):1365–74.
63. Maqbool Z, Asghar HN, Shahzad T, Hussain S, Riaz M, Ali S, et al. Isolating, screening and applying chromium reducing bacteria to promote growth and yield of okra (*Hibiscus esculentus* L.) in chromium contaminated soils. Ecotoxicol Environ Saf. 2015;114:343–9.
64. Islam F, Yasmeen T, Arif MS, Riaz M, Shahzad SM, Imran Q, et al. Combined ability of chromium (Cr) tolerant plant growth promoting bacteria (PGPB) and salicylic acid (SA) in attenuation of chromium stress in maize plants. Plant Physiol Biochem. 2016;108:456–67.
65. Liu C, Jiang M, Yuan MM, Wang E, Bai Y, Crowther TW, et al. Root microbiota confers rice resistance to aluminium toxicity and phosphorus deficiency in acidic soils. Nat Food. 2023;4(10):912–24.
66. Ma Z, Jiang M, Liu C, Wang E, Bai Y, Yuan MM, et al. Quinolone-mediated metabolic cross-feeding develops aluminium tolerance in soil microbial consortia. Nat Commun. 2024;15(1):10148.
67. Acuña JJ, Jorquera MA, Barra PJ, Crowley DE, de la Luz MM. Selenobacteria selected from the rhizosphere as a potential tool for Se biofortification of wheat crops. Biol Fertil Soils. 2013;49:175–85.

Publisher's Note